The Radar "Three-Body Scatter Spike": An Operational Large-Hail Signature

LESLIE R. LEMON

Lockheed Martin Ocean, Radar & Sensor Systems, Syracuse, New York

ABSTRACT

Recently, a rare radar artifact called the "flare echo" or "three-body scatter signature" has been examined by several researchers. Here, this midlevel storm signature is called the "three-body scatter spike" (TBSS) and is examined in detail for some severe storms scanned by operational WSR-88Ds. The TBSS is a generally 10–30-km long region of echo aligned radially downrange from a highly reflective (>63 dBZ) echo core. It is found almost exclusively aloft and is characterized by low reflectivity and is usually characterized by near-zero or weak inbound velocities. Spectrum widths are very broad and often noise like. The aforementioned research concluded that it is caused by non-Rayleigh radar microwave scattering (Mie scattering) from a region of large hydrometeors; most likely large, wet hail. This conclusion is supported and expanded upon.

WSR-88D data are presented concerning a storm attended by a TBSS that produced giant (>5 cm) hail and violent surface winds. In this case, the three-body signature was found in midlevels, down radial from a 65-dBZ reflectivity core in the storm echo overhang. It was most pronounced during 2.5-cm surface hail occurrence and preceded by ~25 min "baseball-size" hail. The signature is shown in base reflectivity and velocity products and in cross sections of reflectivity, velocity, and spectrum width. TBSS theory of production, its appearance, and characteristics are discussed as well as its operational use. Other examples are also examined briefly. Time and location of surface severe weather reports are also examined and related to three-body scattering. The operational interpretation and application to the severe storm warning program are emphasized. It is suggested that the TBSS is a sufficient but not necessary condition for large hail detection. Although all storms examined in this study produced hail >6.5 cm, it is concluded that surface hail of at least 2.5-cm diameter should be expected with artifact-bearing storms. It is further shown that recognition of the TBSS can provide a warning lead time because it typically precedes the largest surface hailfall (and very often violent surface winds) by 10–30 min.

1. Introduction

Zrnić (1987) and Wilson and Reum (1986, 1988) examined a rare radar artifact called the "three-body scatter signature" by Zrnić, or "flare echo" or "hail spike" by Wilson and Reum. Zrnić concluded that it is caused by non-Rayleigh radar microwave scattering from a region of large hydrometeors; most likely large, wet hail. Non-Rayleigh, or Mie scattering, is defined as scattering due to a scatterer whose diameter to wavelength ratio is greater than 1/16th the radar wavelength. When viewed in the context of a vertical cross-section image, flare echo seems a more appropriate nomenclature for the signature; however, in the more typical quasi-horizontal plan position indicator slice through the storm echo, spike seems more appropriate. Here we will call the artifact a three-body scatter spike or simply TBSS. Zrnić derives the theoretical origin for these reflections. He explains and Wilson and Reum (1988) concur that this radar echo feature is the result of triple reflections (a three-body interaction). According to Zrnić, the process consists of 1) forward microwave scattering by strongly reflecting hydrometeors to the ground below, 2) backscattering by the ground to the same hydrometeor region aloft, and 3), in turn, backscattering to the radar. These authors suggest a wavelength dependence with occurrence frequency decreasing with increasing wavelength. For this reason, TBSS signatures can be observed using 5-cm (C-band) radar and are related to large raindrops rather than hail. Here, it is shown that in 10-cm (S-band) WSR-88D base products, the TBSS is found extending downrange behind a reflectivity (>63 dBZ) core in some intense convective storms. In general, all studies including this one found that the signature was almost exclusively aloft, has low reflectivities (<20 dBZ), is relatively short when using modest display thresholds (<~15 km), and is usually characterized by near zero or weak velocities approaching the radar. In order to be seen clearly when it does occur, the area downrange of the storm core should be clear of other echo or storms. The reflectivity core should also be relatively near the down-radial echo edge. The closest range location of the TBSS appears beyond the core of high reflectivity

Corresponding author address: Leslie R. Lemon, Lockheed Martin Ocean, Radar & Sensor Systems, 16416 Cogan Drive, Independence, MO 64055.
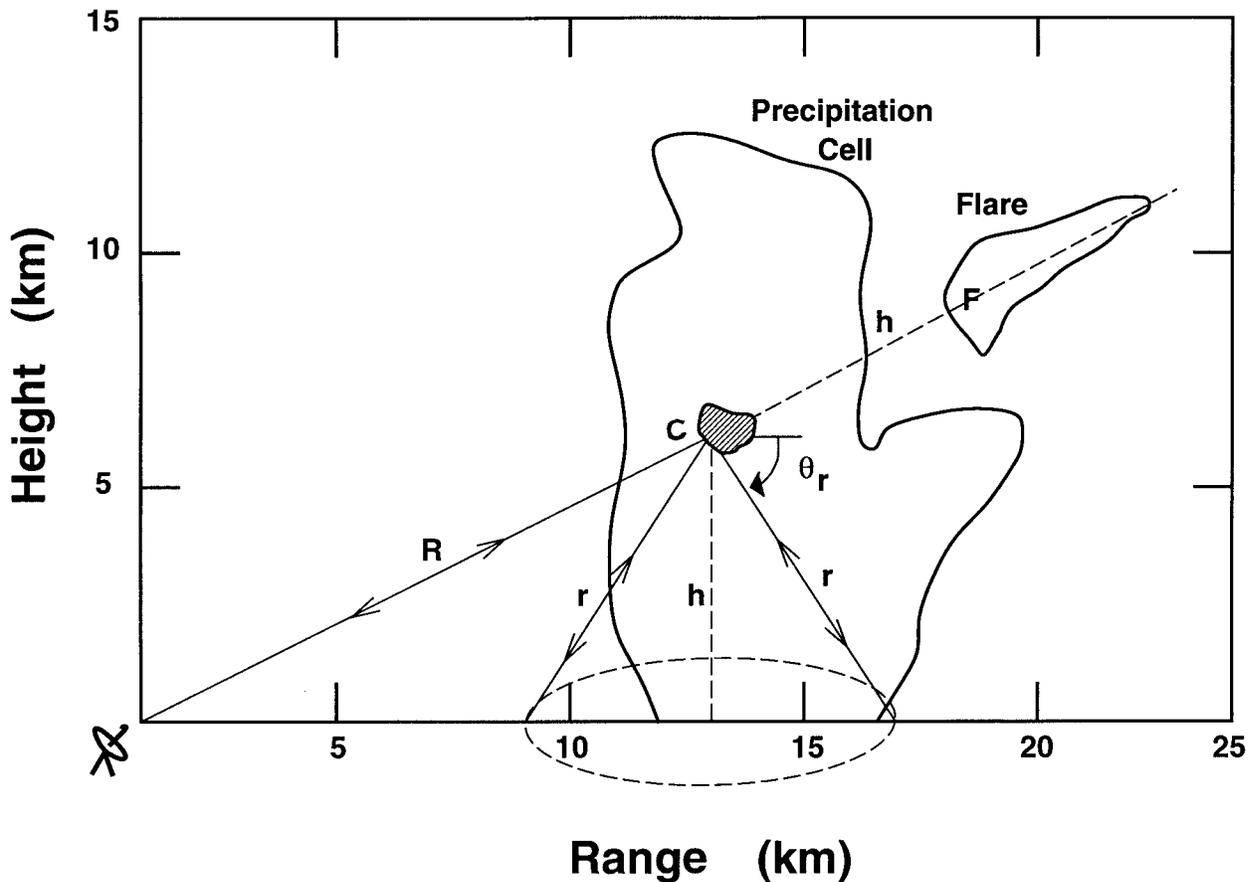E-mail: lrlemon@compuserve.com

FIG. 1. Schematic of the radar signal path responsible for the three-body scatter spike (or flare echo). The dark shading near point C represents the 60+ dBZ core responsible for producing the artifact, from Wilson and Reum (1988).

at a distance equal to the height of the radar illuminated core.

In this paper, the theory of the three-body scatter spike production, its WSR-88D appearance, and characteristics are discussed. One storm attended by such a signature is examined in detail. That storm produced 7.5-cm-diameter hail and $\sim$50 m s^{-1} surface winds. In this case, the most prominent manifestation of the spike is short lived, aloft, radially downrange from a 65–70-dBZ reflectivity shaft in the storm echo overhang, and found during $\sim$2.5-cm surface hail fall. It occurred 28 min before reports of baseball-size surface hail. The signature is shown in base reflectivity and velocity products and in cross sections of reflectivity, velocity, and spectrum width. Additional WSR-88D examples are also shown. Surface severe weather reports are related in time and location with the radar signature in these examples. Finally, conclusions as to the spike's operational use as a large-hail indicator are discussed. It is suggested here that WSR-88D detection of a TBBS is a sufficient but not a necessary condition for large ($>$2.5-cm diameter) hail identification with a storm. However, it is further suggested that when occurring within the storm echo, velocity, and velocity spectrum width contribu-

tions of three-body scattering may obscure or distort images of the internal velocity patterns such as mesocyclone signatures.

2. Theory

For a more thorough theoretical development of the three-body scatter spike, the reader is referred to Zrnić (1987) and Wilson and Reum (1988). As illustrated in Fig. 1, the three-body or flare echo involves a triple reflection of radar microwaves between a region believed to contain wet hail, having diameter-to-wavelength ratios characteristic of Mie scattering, and the ground. In fact, Zrnić concluded that these hailstones are most likely very large solid cores with a surrounding layer of spongy ice having a sizable effective water thickness. Signals follow a path of length R from the radar to a convective storm where they intercept a region of strongly reflecting targets that scatter these signals downward in a manner defining a region of concentric ellipses on the ground beneath (and at slant ranges r) from the scattering volume. The trees, earth, and vegetation reflect the energy diffusely, again illuminating the same region aloft. Zrnić shows that the backscattered

power from the ground drops off as r^{-3}, that is, with the inverse cube of the distance from the region aloft to the ground. For a second time, the region of large targets aloft scatters the power, but this time a significant amount is received by the radar and is amplified and displayed along the original radial. Due to the longer traversed paths of these triple-reflected signals, they arrive at the radar later than the signals, which were directly backscatterd from the core region and thus are seen at longer ranges. Inspection of Fig. 1 reveals that the TBSS echo begins along the radial downrange of the core at a point $R + h$, where h results from a θ_r of 90° corresponding to the height directly above the ground of the original radar scattering volume center. Subsequent range gates displayed at longer ranges along the TBSS are from progressively longer slant ranges (r's), defining larger elliptical areas. However, all scatterers in the reflectivity volume participate in the three-body scattering. Reflected power from a variety of other locations within the illuminated hail region can contribute to each TBSS range gate beyond the gates that receive contributions directly from the ground beneath. Note, of course, that each gate displayed farther outward along the spike will have progressively lower reflectivities because of the r^{-3} decrease of power with distance from the scatterers. Therefore, the first gate in the three-body scatter spike will have the maximum reflectivity. Because signals are transmitted and received along the same radial but with longer traversed paths, the resulting three-body echo is displayed as a radial spike downrange from the reflectivity core. This echo spike is strictly an artifact; in reality the responsible reflectors do not actually exist at the locations displayed along the TBSS although their range is correct. Depending on the beamcenter height through the strongly reflecting region, the TBSS will begin at various downrange locations from the core. The higher above the ground the radar scan intercepts the strong echo core, the farther away from the core position will the first artifact gate appear. This is why the illustrated flare begins at point F that is ~7 km downrange, equal to the height of point C. Thus, in this case, the flare begins outside of the "precipitation cell" or radar echo in Fig. 1. Moreover, if the radar elevation scan of the hail region is very near the earth's surface, the spike will probably not be detected at all. This is because the TBSS will begin immediately behind the echo core and when it reaches the echo edge it may be too weak to display, that is, less than the display threshold (5 dBZ). Five dBZ is the lower bound reflectivity display threshold for the WSR-88D when in precipitation mode. Any reflectivities less than this are currently not displayed in image products.

This lower-bound reflectivity threshold of 5 dBZ has other ramifications. Wilson and Reum (1988) find the TBSS signature commonly characterized by maximum reflectivities of ~20 dBZ as are most of those identified by the WSR-88D. However, these values are in the first range gate as explained above and often overlay actual precipitation echo and are therefore indistinguishable. Moreover, they often find that the spike extension downrange is characterized by reflectivities as low as −10 dBZ; these values are not now displayed on the WSR-88D products when in precipitation mode. The WSR-88D signatures, when detected extending outward from the main echo body, are typically 5–10 dBZ. If the minimum displayed reflectivities were lowered in the precipitation mode, the spike would be longer and probably detected more often. The operational importance proposed in section 5 of these weaker signatures might be altered because they would be detected more easily and more often.

Zrnić proposed that the measured, mean velocities displayed along the three-body echo are functions of the radial and vertical motions of the hydrometeors in the region at point C (Fig. 1). He proposed that the dominant function can be approximated by $W \sin\theta_r + U$ where W is the vertical speed of hydrometeors and U, the radial component of the velocity at the location of the scatterers. However, Zrnić, (1997, personal communication) also suggests that the velocity spectrum was broadened considerably due to the function of $U \cos\theta_r$ and ground reflections. Further, each location along the TBSS is also defined by scattering from a variety of locations within the hail region and for a variety of θ_r's, all of which produce the same pathlength. Thus, the velocities attributed to each location are, in fact, averaged components of W and U from a variety of locations within the hail region. The only point where the radar estimated velocity simplifies is at the mirror point. We expect, and the data verifies, that resulting spectrum widths are very broad because they contain, from a variety of hail region locations, contributions by fall speeds and radial speeds as well as some contamination by vegetation and other ground target motions.

Hailstone growth takes place in midlevels most rapidly within updraft where there is an abundance of supercooled liquid water. Furthermore, these updrafts, which promote the growth of very large hail, are most often intense, large, and less affected by mixing with environmental air aloft (Browning 1978). Thus, these growing hailstones are being carried across the updraft by the conserved, low-level, horizontal momentum feeding the updraft from below. For this reason the Doppler detected horizontal velocities, U, in the hail region will have a component of the low-level storm inflow. Furthermore, U will vary in sign depending on the viewing angle of the radar.

However, because the hailstones responsible for three-body scattering are large with correspondingly large terminal fall velocities, W is nearly always negative except within extremely intense updrafts. Therefore, the quantity, $W \sin\theta_r + U$, is most often negative to some degree but moderated by the influence of ground targets and, potentially, by U. At least in part for these reasons, it is expected that TBSS signatures are dominated by weak negative velocities. But, for the special

case of the mirror point, where θ_r is 90°, the measured velocity will be essentially $W + U$. Because U is measured within the reflectivity core and hail volume itself, W can be estimated. Using this special condition, Wilson and Reum (1986), in one case, inferred the development of a microburst within a reflectivity core. But, because the mean velocities in all but the mirror point are derived from generally broad and, sometimes multimodal or nearly flat spectra and often dominated by ground reflectors, they are of little operational use.

A potential problem exists most often in the near-surface elevation scans through the hail shaft. In these cases the velocity contributions from the TBSS can occasionally contaminate in-storm measured velocities. However, reflectivities within the spike, while initially relatively high in the near-ground scans, will weaken rapidly as the downrange distance from the core increases. Thus, potential contamination will generally be confined to short distances downrange of the core. The problem will be most critical when a scanned low-level mesocyclone is immediately downrange of a hail core. In view of established supercell storm structure, this is not an unusual situation (Lemon and Doswell 1979). As mentioned, owing to the very short TBSS length in near-surface scans, the existence of the spike may not be detected at all because it will be wholly contained in the precipitation echo. Finally, although velocity field contamination may be suspected (as in a later example), it will be difficult to verify, especially without use of spectrum width information.

As stated earlier, the highly reflective region intercepted by the radar beam and causing substantial three-body scattering is interpreted to be large hail. Wilson and Reum (1988) conclude that in Colorado the three-body scatter spike (flare) and 2.5-cm or larger diameter surface hail are highly correlated for S-band radar. They cite TBSS cases where exceptionally large quantities of hail produced significant surface accumulations. Zrnić also provides a convincing argument that these hail stones have a substantial water coating. Because dry hailstones of equivalent size backscatter ~7 dB less power due to the difference in the complex index of refraction for ice and water, they are probably not responsible for three-body scattering. Atlas and Ludlam (1961) show that melting ice spheres would be expected to have a maximum water coating depth of only 0.1 mm before shedding the excess water. Maximum scattering can be expected from ice spheres coated with a layer of spongy ice having a substantial (10%–15%) liquid water mass. In fact, Browning et al. (1968) and Summers (1968) point out that, invariably, the larger stones have a higher liquid content and are those that tend to be spongy.

Although Zrnić states that in the case he examined the three-body scatter artifact did not occur substantially above the freezing level, here we find evidence for wet hail growth and spongy hail well above the freezing level. This is consistent with hail growth studies (English 1973). With the exception that many signatures are found far above the environmental freezing level, results here confirm Zrnić, and Wilson and Reum's findings. In fact, although there are not a very large number of WSR-88D examples documented thus far, *in most cases,* hail of at least baseball size has been reported with the WSR-88D, TBSS-associated storms. It is too early to claim that those storms producing this artifact are *only* baseball hail producing storms. Indeed, a few TBSSs have been found with storms having hail significantly smaller than 5 cm in diameter. However, at least in the high plains, studies (e.g., Wilson and Reum 1986, 1988; Lemon 1994) suggest that storms with the TBSS are likely to produce hail having diameters of *2.5 cm or greater* or very large quantities of lesser hail. (It is also noteworthy that the majority of these storms are also damaging wind producers.)

3. The Cashion storm

The Cashion, Oklahoma, storm exemplifies the WSR-88D TBSS. For greater detail concerning this storm, its environment, its characteristics, and other storm findings, see Lemon and Burgess (1993) and Burgess and Lemon (1993).

A weak, nearly stationary front extended across the northern Oklahoma counties on 18 June 1992. South of the front the atmosphere was extremely unstable (convective available potential energy of 4000–6000 J kg^{-1}, lifted index of ~ -14) but with weak dynamics. The 5–8 m s^{-1} low-level winds veered from southerly at the surface to southwesterly at 3.7 km. A high-level, subtropical jet stream was nearby, attended by 39 m s^{-1} west-northwesterly winds at the tropopause. Locally accelerated surface-inflow winds, apparently in response to the Cashion storm updraft, were found to markedly increase during initial storm formation. The storm developed during the late afternoon (2137, all times UTC) in an east–west towering cumulus line detected by the central Oklahoma WSR-88D (KTLX) and moved south-southeast ($\sim 325°$, 10 m s^{-1}). The accelerated surface winds produced storm-relative helicity of ~ 290 m^2 s^{-2}. This value was well above that needed for mesocyclone formation (Davies-Jones et al. 1990).

a. Storm evolution

During Cashion storm observation, the radar was operated in volume coverage pattern (VCP) 21 that employees nine elevations scans during each 6-min volume scan (NOAA 1991). VCP 21 scans at elevation angles 0.5°, 1.5°, 2.4°, 3.4°, 4.3°, 6.0°, 9.9°, 14.6°, and 19.5°. The lowest five scans are contiguous but a 0.7° gap exists between the 4.3° and 6.0° scans.

Following the appearance of the first echo at an elevation angle of 4.3° and a height of ~8.2 km [all heights are above ground level (AGL)], the storm increased in intensity and height rapidly. It developed an
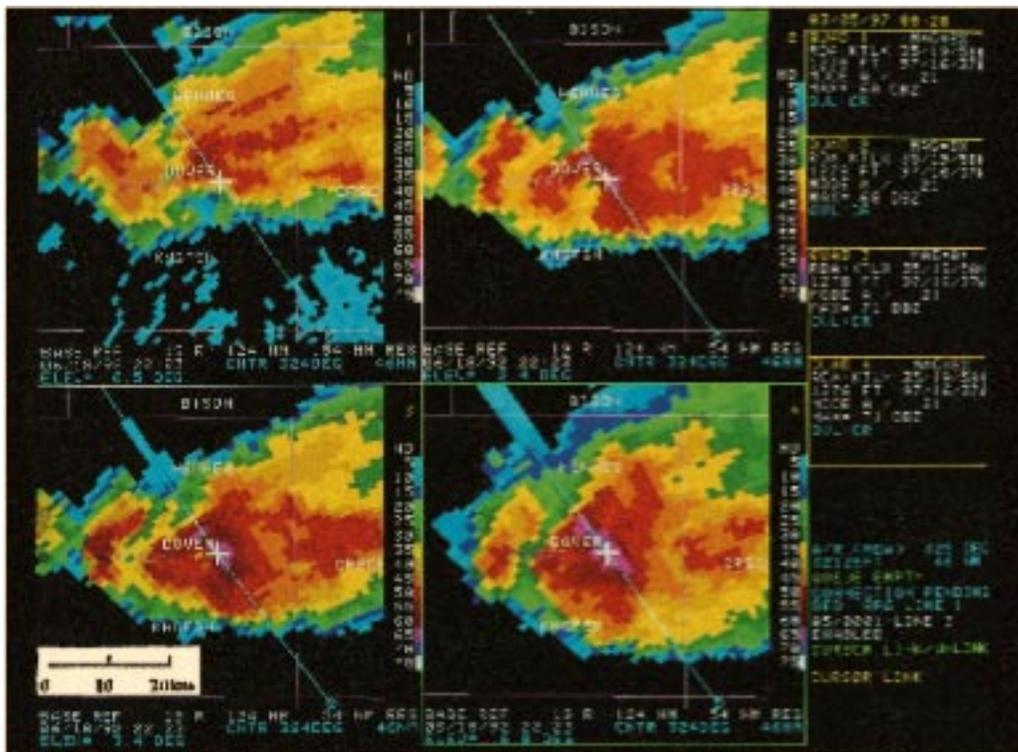
FIG. 2. WSR-88D quarter-screen reflectivity display from the Cashion, OK, storm. Images are magnified eight times; data resolution is 1 km (0.54 nmi). Radar data elevation angles are upper left, 0.5°; upper right, 2.4°; lower left, 3.4°; and 6.0°. Vertical cross-section axis location corresponding to Fig. 3 is shown in each image. The cursor is located on the reflectivity core responsible for three-body scattering and the cross section axis extends through the TBSS to the storm rear in 2.4°, 3.4°, and 6.0°.

overhanging reflectivity region and resulting weak echo region (WER), with echo top above the WER. The radar and visual appearance of this storm suggested the presence of an intense updraft; it appeared to be a supercell storm. Lemon (1978) showed these radar structural features are indicative of hailstorms. By 2206, in the 4.3° elevation scan at ~7.6 km where reflectivities had reached 64 dBZ, the first three-body scatter spike appeared. In only 35 min after first echo, at 2212, the storm had developed a bounded weak echo region (BWER), midlevel mesocyclone, a 77 kg m^{-2} vertically integrated liquid water (VIL), and 70-dBZ reflectivities at ~7.0 km. Though subtle, the TBSS also became apparent at 3.4° (~5.2 km) as well as 4.3° (~7.0 km) elevation scans. The midlevel radar artifact continued through the 2253 volume scan. Most obvious and striking was the TBSS signature observed during the 2223 volume scan (Figs. 2 and 3).

Throughout the remaining analysis period ending at 2310, the storm maintained a mesocyclone, BWER, and occasional low-level hook or pendant echo as it moved south-southeast. Familiar supercellular reflectivity structures of echo overhang, WER and BWER, are easily recognized in Figs. 2 and 3. The moderately intense mesocyclone remained mostly aloft while brief small but radar detectable vortices would spin up along the low-level gust front. One of these produced a brief tornado, sometimes referred to as a "gustnado," at 2241 along the gust front and was photographed by meteorologist/field observers. Near 2300 the broader-scale mesocyclone penetrated to the lowest radar elevation scan, abruptly strengthened (reaching a 23 m s^{-1} rotational velocity), and extended vertically to a depth >10.7 km simultaneously with the development of a microburst and downburst. It was also at this time that a tornadic vortex signature (TVS) appeared at 6.7 km AGL. During the next 10 min, the TVS extended upward but, apparently, was not associated with a surface tornado.

In association with the surface mesocyclone spinup and downburst development, the town of Cashion experienced winds estimated at up to 51 m s^{-1} and extensive damage. Damage estimates were upwards of $1 000 000. Although moving through a relatively unpopulated area, a total of nine severe weather reports were received. In addition to the tornado and Cashion wind storm, other damaging winds over 36 m s^{-1} were reported. Several surface hail reports ranged from 1.9 cm at 2220 to 7 cm near 2300.
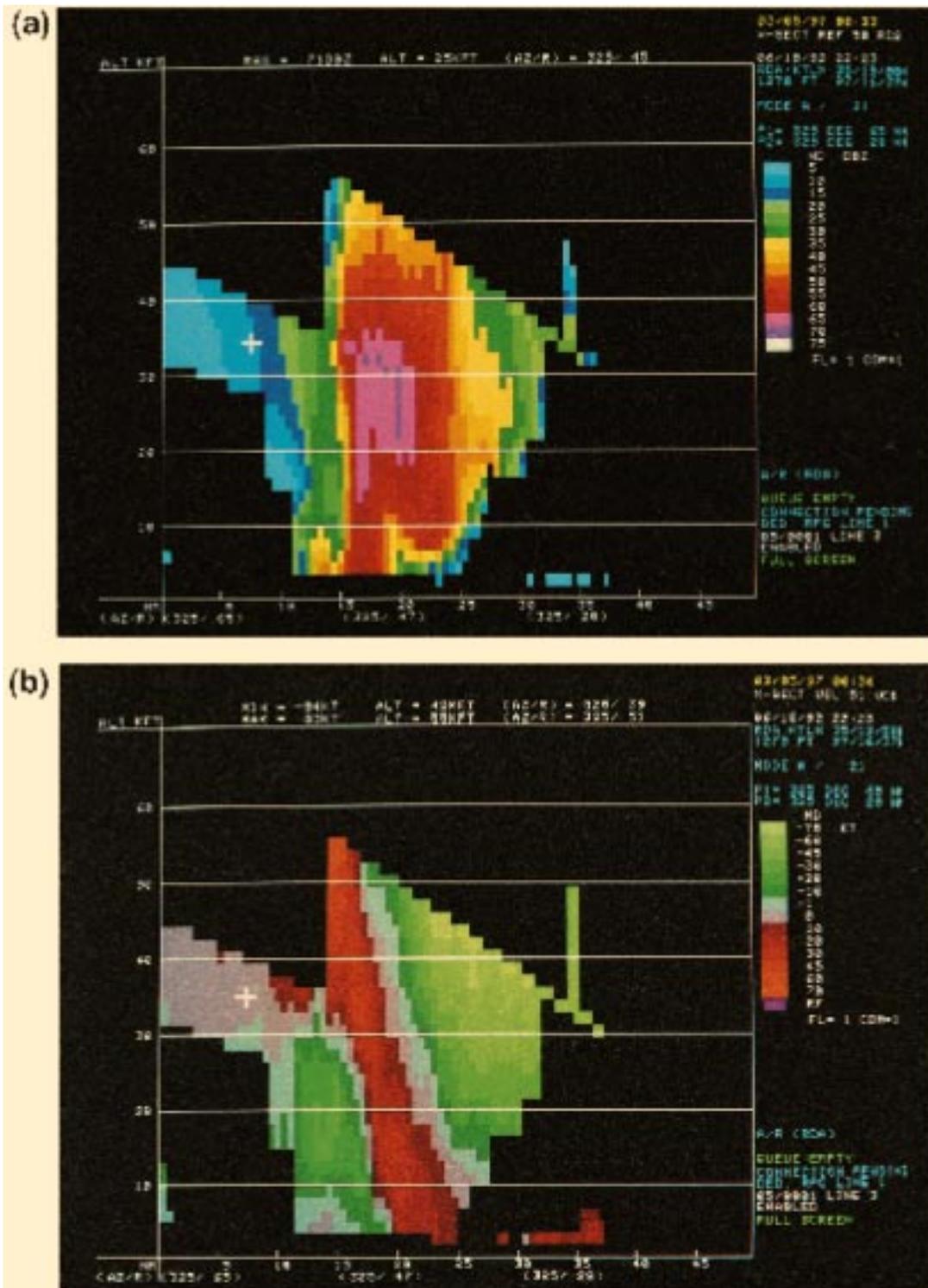
Fig. 3. WSR-88D vertical cross sections of (a) reflectivity, (b) mean radial velocity, and (c) velocity spectrum width generated along the axis shown in Fig. 2. The radar is located toward the right side of each cross section display. Note the cursor is located on the TBSS beyond the trailing edge of the storm. (Note that units are English. To convert heights to meters, divide by 3.281, and to convert horizontal distances to kilometers, multiply by 1.853.)
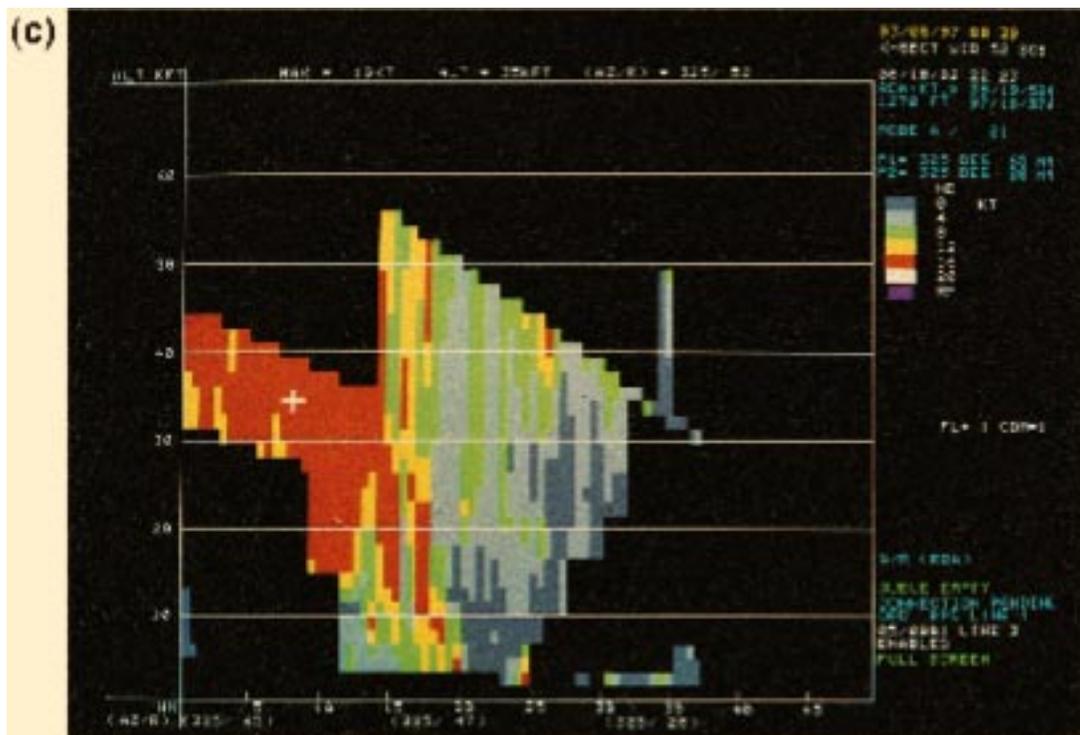
FIG. 3. (*Continued*)

b. Cashion storm three-body scatter spike

As is typical, the Cashion storm TBSS was confined to midlevels, between 4.3 and 9.8 km. Thus, those elevation cuts that exhibited the TBSS during the analysis period involved those between and including 2.4°–6.0°.

The signature was not observed in the lowest two scans even though the hail shaft extended to the surface. It is believed that this was true for two reasons. First, the bulk of the parent-storm echo mass was to the northwest (downrange) of the echo core. The three-body scatter spike begins downrange from the core at the point $R + h$. Because the range to the storm is relatively small, less than 93 km, h is minimal, between 1.2 and 3.0 km. This translates into a distance from a radar gate producing three-body scattering to the mirror point 1.2 km and 3.0 km down range, respectively. This distance is well inside the echo body. Then, for the larger ranges of $R + r$, as r increases, the reflectivities drop off rapidly and are less than 5 dBZ near the actual back edge of the storm echo. Second, a substantial amount of liquid water may be contained aloft in a spongy ice shell surrounding the developing hailstone. If so, much of that shell may melt away during the final descent through the near-surface layer of quite warm, moist air. The result is a hailstone that has aerodynamically shed much of the water, leaving a solid ice sphere with little water coating. This is significantly less reflective and less effective as a three-body scatterer. This possibility is further supported because, for a noticeable three-body scatter spike to occur in the Cashion storm, a reflectivity threshold of >63 dBZ was observed and apparently required. Values at 0.5° only exceeded this apparent threshold once and that during the 2229 volume scan.

Three-body scattering was not observed in this case at elevation angles higher than 6.0°. At 2223 the 6.0° elevation angle intercepted the storm core at 9.8 km. Microphysical hail growth studies have found wet growth can and does take place at these altitudes with temperatures less than −30°C (English 1973). However, after this time in the Cashion storm, three-body scattering was never observed at comparable heights. This later absence of three-body scattering above ∼8.5 km is attributed either to the absence of hail or to only dry hail growth at those altitudes. Although soundings from the Oklahoma City Weather Service Forecast Office were not available on that day, judging from synoptic charts, temperatures were likely between −35° and −39°C in the still buoyant (by a few degrees Celsius) updraft at about 10 km. Thus, at 2223, and ∼9.1 km AGL, apparently spongy, liquid water containing hailstones existed, at least briefly. English (1973) found that in studying a number of storms, the two that produced the largest hail attained largest liquid water content and updraft strength with updraft temperatures of ∼−38°C, at about this altitude. Further, she found that hail production was often unsteady, even in supercellular storms. This is consistent with the later absence of three-body scattering (and large, wet hail) at this altitude.

While the Cashion storm exhibited the TBSS for 47 min, we examine the artifact in detail during the 2223 volume scan because of its obvious appearance (Figs. 2 and 3). At that time the signature was observed from 2.4° (~4.0 km) through 6.0° (~9.1 km).

The very large, highly reflective region producing the TBSS occupies a portion of the storm normally dominated by updraft and rapid hail growth. That conclusion is supported by the presence of an extensive echo overhang, associated substantial WER, and BWER, beneath much of the echo core. Echo summit and divergence are found above. The only portion thought not to be upheld by this draft is the shaft extending downward toward the storm rear in the "wall" (Browning 1964) where the leading edge of the precipitation cascade region, hail, and downdraft are located. All this is further supported by derived vertical motions in the reflectivity core region (briefly discussed below). Lemon and Burgess (1993) and Lemon and Parker (1996) showed that the nearly vertical deep convergence zone within the wall separates leading intense updraft (characterized by outbound velocities) from trailing downdraft (characterized by inbound) velocities (Fig. 3b).

At 6.0° elevation, the TBSS is very obvious along the 325° and 326° radials (Fig. 2). Within the storm core, along the 325° radial, approximately 12 km of 65 dBZ or greater reflectivities are encountered. Reflectivities of 70 dBZ extend over 3.7 km in range along this radial. As concluded from inspection in this case, detectable three-body scattering is produced by reflectivities that exceed 63 dBZ along the radial. The point examined here for emphasis is the last gate with 70 dBZ. Beam height at that range location is ~9.8 km AGL. Thus, the mirror point will appear ~9.8 km radially downrange. There, reflectivities are between 25 and 30 dBZ and may include returns from actual precipitation as well. Downrange the TBSS with decreasing reflectivities is ~31.5-km long. As is typical, reflectivities of 15 dBZ or less dominate most of the spike. In the adjacent azimuth, 326°, the spike is ~24-km long. Similarly, at 3.4°, or 6.4 km AGL and 325° azimuth, the spike is ~15-km long involving reflectivities less than 15 dBZ. The adjacent 326° azimuth is characterized by a spike 5.6-km long. The TBSS in many other storms seen by this author is less than about 15 km when using a display threshold of 5 dBZ.

As pointed out earlier, the TBSS mirror point (F, Fig. 1) is a point where measured radial and vertical motions from the original scattering volume are displayed in combination. The scope of this paper does not allow vertical velocity derivation in any detail nor substantial discussion. However, indications are that those hailstones in the core volume near 9.1 km AGL are only relatively slowly subsiding (having a fall speed of ~−13 m s⁻¹) while they are carried rapidly (~38 m s⁻¹) in a storm relative sense from right to left across the updraft toward their descent in the precipitation cascade region, downdraft, and reflectivity gradient (Figs.

3a,b). Here, at ~9.1 km, rapid wet hail growth is taking place within updraft roughly estimated at ~25 m s⁻¹. In contrast, at lower elevation angles in the cascade region, hailstones are believed to be falling at or near their terminal fall velocities through the deep convergence zone adjacent to the updraft.

The spectrum width signal provides some additional interesting information about the TBSS. Figure 3c shows that the velocity spectrum width is quite large. This is a result of the presence of a complex mixture involving both horizontal and vertical motions of the scatterers in this region. The combination produces a very broad, sometimes noiselike spectrum width signal. Note that if the relatively low-power, noiselike TBSS overlays weak, but real storm echo, the velocity will be contaminated from the combination of the real and artifact velocities. In this case (see Fig. 3b), the substantial velocity continuity within the storm boundary suggests that the velocities in the storm along this radial are fairly reliable, so TBSS velocity contamination does not seem to be present.

c. Association with severe weather

An attempt is made to establish surface severe weather occurrence with three-body scattering in an effort to evaluate the operational implications of the signature. However, two problems are confronted. First, there is the problem of population density and reporting. The Cashion storm was passing through a relatively unpopulated rural area during the analysis period considered here. Storm development occurred south of Hennessey and just east of Dover (both towns of less than 3000 people). Although the town of Kingfisher is the county seat, the storm was largely to the northeast, passing through open country until encountering the hamlet of Cashion. Thus, relatively few people experienced or were available to report severe weather. A minority of those who do experience severe weather report it. An advantage in this case was meteorologists/observers who maintained positions ahead of the storm. But they deliberately avoided the precipitation area owing to its safety and mobility threat. Second is the problem that three-body scattering occurs when the radar beam encounters developing hail aloft. This hail has yet to reach the ground. Various studies indicate that developing-hail resident times in a storm range from ~10 min to over 35 min with the longer times for larger stones.

The first surface report for hail of 1.9-cm diameter was at approximately 2220 from beneath the developing storm core. This was about 14 min after the first subtle three-body scatter spike associated with a reflectivity core within the updraft appeared at ~7.3 km and just prior to the most prominent three-body scattering with this storm. After a brief tornado and a damaging wind occurrence it was not until 2251 that 4.4-cm hail was reported along the leading reflectivity gradient adjacent to the updraft. For the next 15 min several reports of
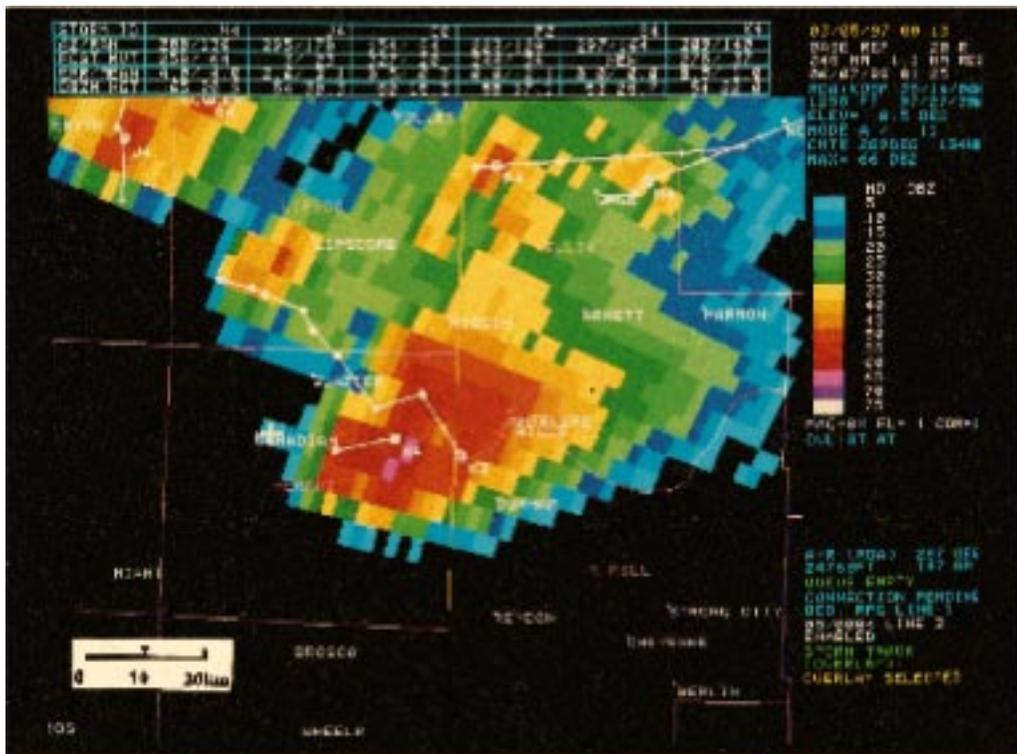
Fig. 4. Severe thunderstorm WSR-88D reflectivity image with a resolution of 1.1 nmi (2 km), 7 June 1989 at 0.5° antenna tilt, with storm track information overlay. The storm is ~289°/135 nmi (250 km) from the radar. Note that the cursor is located on the TBSS downrange of the southernmost 65-dBZ reflectivity core within the storm located in eastern Hemphill County, Texas.

very strong damaging winds and baseball-sized (~7 cm) hail were reported. Many of the other reports were also received from the same storm-relative location, just behind the gust front, BWER, and major storm updraft that is, in the cascade region. Reports of baseball-size hail ceased after about 2305, although subsequent reports of lesser hail were received. Observations of three-body scattering, again subtle, were last noted at 2253. [Archived base data (Crum and Alberty 1993) are not available after 2310. Therefore, analysis beyond that time was not possible.]

Accounting for ascent and resident time in the updraft and hail descent, most of these reports correlate well with radar three-body scattering aloft. Baseball-size hail as well as damaging wind reports followed the most pronounced three-body scattering by about 30 min. Although hail growing rapidly and moving across the updraft at 2223 would have probably arrived at the surface 10–15 min earlier than reported. Due to pitfalls of event occurrence, observation, and reporting, the lack of large hail reports between 2230 and 2245 should not be interpreted as absence of large surface hail. Note that the implication is for an operationally *predictive* capability at the ground using the TBSS detection aloft.

4. Other examples

No systematic review of WSR-88D data archives to statistically find and correlate three-body scatter spikes with large hail or any other severe weather has been undertaken. Nonetheless, a cursory review of limited available data and 1995 and 1996 real-time observations reveal that WSR-88D three-body scattering is not extremely rare. Many other cases have been less dramatic and more subtle, but easily recognizable when TBSS characteristics are known and the observer is alert to their possibility.

a. Case 1

In his theoretical three-body scatter derivation, Zrnić found that the artifact is independent of radar range to the scattering volume if certain conditions are met. These conditions are 1) the scatterers fill the beam, 2) their scattering does not depend strongly on direction, and 3) the ground scatters almost omnidirectionally. In our first example (6 June 1989), the first condition is questionable. The storm's 66-dBZ scattering volume was 250 km away (Fig. 4). At that range the Operational Support Facility WSR-88D beamwidth is over 3.6 km.
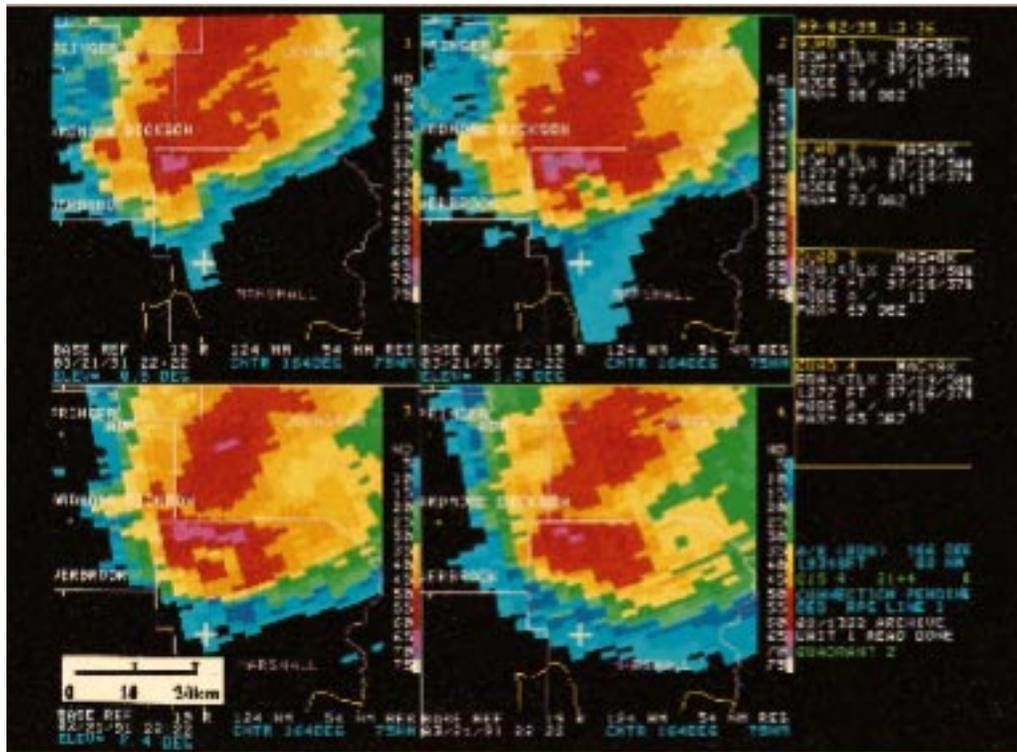
FIG. 5. The 21 March 1991 Base Reflectivity quarter-screen products, 1 km (.54 nm) resolution. Elevation angles are: upper left, 0.5°; upper right, 1.5°, lower left, 2.4°; and lower right, 3.4°. Cursor is positioned on the TBSS in the first three quadrants. Note the 65-dBZ echo core and the resulting TBSS passing through the mesocyclone associated pendant echo and farther downrange.

Perhaps because the storm was of great depth (~20.1 km top), large, and supercellular, three-body scattering was observed even without beam filling. If beam filling is indeed required, then there would appear to be a range dependence.

This case was during the Next Generation Weather Radar (NEXRAD) Interim Operational Test and Evaluation in Norman, Oklahoma, when archive level II data were collected. Particularly severe storms developed and have, in part, been documented by Burgess and Lemon (1991). The storm in question in Hemphill County, Texas, was producing surface hail ranging in size up to 10 cm and had produced a tornado during the time of interest.

As seen in Fig. 4 (but somewhat subtle), an 8.5-km-long three-body scatter spike was observed downrange from the storm reflectivity core of 66 dBZ at 7.0 km AGL. The core was adjacent to a detectable BWER. Although this scan is 0.5°, at that range it intercepts the storm at midlevels.

b. Case 2

Just one day after an operational assessment of the KTLX WSR-88D began, an outbreak of severe storms struck the state of Oklahoma on 21 March 1991. One of those storms produced multiple mesocyclones, wind

damage, large hail, and at least one tornado (Fig. 5). At 2222, a TBSS of ~20 km length (reflectivities <20 dBZ) was observed at ~4.3 km AGL. Reflectivities in the scattering core were between 60 and 72 dBZ. To a lesser extent the artifact was also observed at lower heights of ~2.4 km and at higher altitudes of 7.0 km. Hail up to 4.5 cm had been reported with the storm prior to this time, and 7-cm hail was reported 23 min later. Damaging 4.5-cm hail covering the ground and winds of 40 m s^{-1} were also reported. This signature lasted at least 49 min but the most pronounced three-body scattering was observed during this volume scan.

The mirror point and TBSS passed through the western portion of a mesocyclone within the storm body. Although apparent velocity field disruption was observed, an associated mesocyclone was still identified by the WSR-88D algorithm and manually identified during this period. The mesocyclone was highly asymmetric because the radar-outbound portion of the signature through which the spike passed had only weak outbound velocities. It cannot be determined with certainty that the spike is the cause of this pronounced asymmetry. However, the expected inbound or negative TBSS velocity component overlaid on the outbound velocities of the mesocyclone would have produced just such an effect.
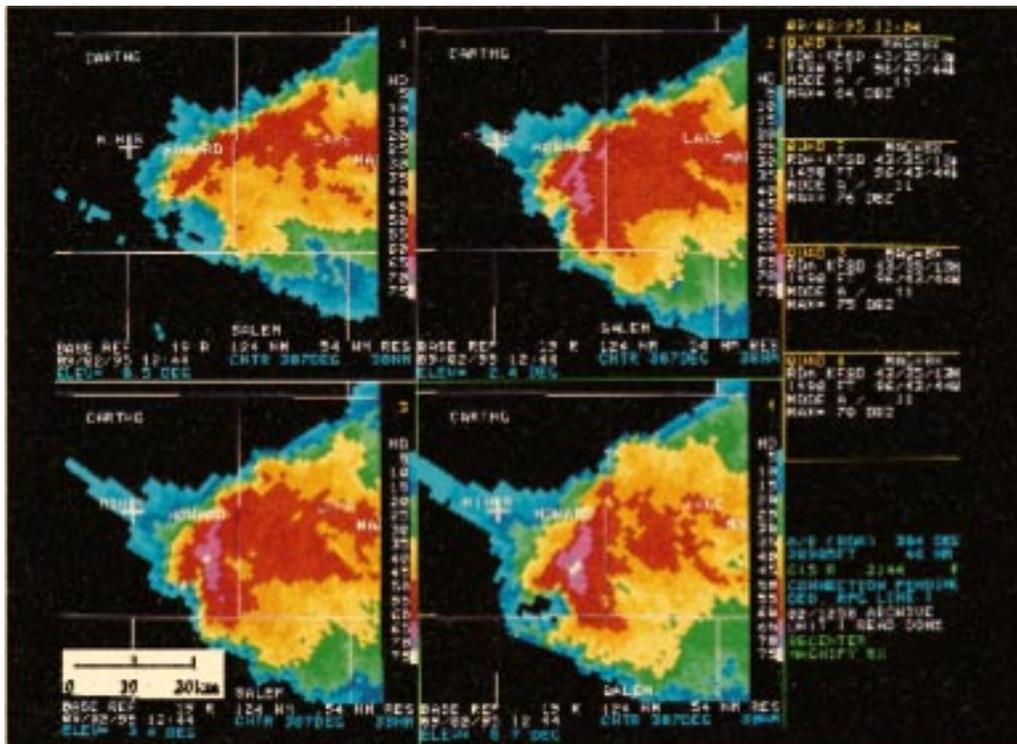
FIG. 6. Quarter-screen, 1-km (0.54 nmi) resolution, base reflectivity products from Sioux Falls, SD, recorded on 2 September 1995 for 0.5° (upper left) and, clockwise, 2.4°, 3.4°, and 5.3°. Cursor overlays the TBSS.

c. Case 3

A severe thunderstorm complex developed in the early morning hours over southeast South Dakota and moved southward. The storm produced four episodes of hail exceeding 6 cm. Prior to each one of those, distinct TBSSs were observed aloft. About 15 min prior to one of those periods during which 4.5–11-cm hail and extensive damage was reported, distinct three-body scattering was observed from ~2 km AGL up through at least 7.6 km (Fig. 6). As can be seen in the region of hail growth, and perhaps not surprisingly for a storm producing such large hail, reflectivities through the same column ranged from 64 dBZ at 2 km up to an extreme of 78 dBZ at 7.6 km. This same storm also produced periods of damaging winds. The storm in Fig. 6 was centered ~70 km northwest of the radar.

5. TBSS operational application

Fortunately the TBSS signature is not merely an esoteric curiosity in radar meteorology, but appears to be a valuable operational and warning tool. Following the initial suggestion by Lemon (1994) and using the work of Zrnić and Wilson and Reum, and this study, important applications are strongly suggested.

First, we consider the circumstances that control the detectability and extent of the TBSS and its limitations. Signature length and strength are directly related to re-

flectivity core intensity (Eyerman-Torgerson and Brown 1995) and to the vertical extent of the reflectivity core. As discussed earlier and pointed out by Eyerman-Torgerson and Brown, the shortest path traveled in the three-body scattering process is from the illuminated hail core, down to the ground and back to the same hail region aloft before being scattered back to the radar. This produces the shortest time delay and, therefore, the earliest TBSS return, and closest point of the signature to the radar (the mirror point). Therefore, as the elevation angle of the radar beam increases, the minimum three-body scatter distance increases, as do all other scattering paths associated with that scan. Thus, TBSS length increases with increasing height. For low to moderate storm ranges (<~120 km), the TBSS signature will usually be confined to midlevel scans because it is here where rapid, spongy, large hail growth takes place and because in low levels, much of the signature is masked by the actual radar return from the storm. Proximity of the core to the echo edge and the presence or absence of downrange echoes from the storm also dictate whether the feature can be discerned. Radial and azimuthal core extent are also important factors to TBSS production and detection. The larger the highly reflecting core area, the more extensive the three-body scattering.

Results obtained here and by other studies using S-band radars indicate that the reflectivity core intensity

must exceed ~60 dBZ. Results by inspection using the Oklahoma WSR-88D radars suggest values >~62 dBZ. [Interestingly, English (1973) points out that in the storms she studied and modeled "rain contents of 10 gm m⁻³ (equivalent to a reflectivity of about 62 dBZ) were necessary to increase *substantially* the ... hailstone sizes."]

Finally, as is the reflectivity core intensity, the intensity and length of the TBSS is a function of the hail size and perhaps hail density (number of stones) in the scattering volume. This is supported by observations of 7-cm diameter surface hail with WSR-88D TBSS's in this study.

One note of caution is appropriate. It should not be concluded that storms producing the artifact, especially the shorter and less obvious signatures, will or are now, *with absolute certainty,* producing very large hail. While large hail or very large quantities of hail aloft are indicated with certainty, significant melting can occur during descent to the surface. Both the temperature and wet-bulb zero temperature may be well above 0°C through a significant portion of hail descent. Thus, if the signature is detected at extreme heights and substantial melting during hail descent is suggested by the sounding, then hail of only 2.5 cm (or in rare cases, even less) may actually reach the surface. Once again, the forecaster must use all environmental information available for warning issuance. An aviation threat due to large hail is certain even in these situations, however.

Nevertheless, with the weight of the studies by Zrnić, Wilson and Reum, and ours, it would be prudent for operational forecaster using the WSR-88D to interpret the signature as indicating hail greater than 2.5 cm in diameter is falling or will fall with the storm. *The three-body scatter spike is a sufficient but not necessary condition for large hail identification.* Therefore, if a warning has not already been issued (most often many other warning criteria will have already been reached), then detection of a TBSS should warrant a warning for large hail. In cases of pronounced TBSS signatures, hail >5 cm in diameter should be anticipated. Furthermore, although reports from a signature-bearing storm may not indicate significantly large hail at the time, it probably is occurring or will occur. When the most pronounced TBSS is occurring, VILs are often very high or increasing. In the Cashion storm the VIL reached 77 kg m⁻² by 2223 and continued to increase to 103 kg m⁻² by 2235. Subsequently, values slowly subsided to 81 kg m⁻² by 2305 when baseball-size surface hail and violent winds were actually being reported. High values of VIL and pronounced three-body scattering very often precede surface hail falls. Both VIL and the TBSS have *predictive value* in that they often develop during hail growth aloft and *before very large hail reaches the surface.* With the correlation of very large hail and often violent winds with the most striking signatures, in these cases TBSS detection should suggest stronger wording in the resulting warning.

It is also noted that all but one of the TBSS storms examined in this study are also known to have produced damaging surface winds. In fact, the winds have been particularly violent, approaching 50 m s⁻¹ in several storms. Three of the storms were associated with F1 to low F2 nontornadic wind damage, and a fourth produced two measured wind gusts of 51 m s⁻¹. This fact is also consistent with observations by Ohno et al. (1994) indicating that the most damaging microburst winds in Japan are almost exclusively associated with hail producing storms. Further, several of these TBSS storms in this study have been found to possess the deep convergence zone (DCZ) characteristics that appear to promote both large hail growth and intense downdraft and damaging surface winds (Lemon and Parker 1996). Several other studies implicate evaporating and melting graupel or hail in downdraft or downburst production, (e.g., Hjelmfelt et al. 1986; Srivastava 1987; Wakimoto and Bringi 1988, and others). Despite the limited dataset, this association suggests that TBSS producing storms should also be anticipated as damaging wind producers.

While the TBSS is certain to be a hail indicator, it must not be construed as hail actually reaching the surface beneath the echo spike itself. This is a scattering artifact indicating precipitation echo where, in reality, none exists.

As always, it is essential that higher elevation-angle base products be used to not only interpret adequately three-dimensional storm reflectivity and velocity structure, but also to detect the TBSS. Although we have used vertical cross sections to illustrate the artifact characteristics, normally the feature is recognized on midlevel base reflectivity and spectrum width products. As in the Cashion storm, the radar artifact is nearly always found during storm midlevel scans. Definition of midlevels is regionally, seasonally, and storm dependent. Base products most commonly used for TBSS identification include reflectivity, velocity, spectrum width, and severe weather analysis. A quarter-panel product displaying reflectivity products for 0.5°, 1.5°, 2.4°, and 3.4° for storms at moderate to long ranges could be used effectively. Vertical cross sections must be *precisely* placed to reveal the critical storm structural features such as the WER, BWER, DCZ, or TBSS and may, therefore, not be as useful for real-time detection.

Spectrum width products are rarely used operationally, but in this context, they are extremely instrumental in confirming TBSS existence or in identifying velocity contamination of interior storm features such as possible mesocyclones. The normal location of reflectivity cores relative to mesocyclones will occasionally result in velocity pattern distortion. Spectrum width can be used to help identify such a distortion.

6. Summary

The three-body scatter spike is a radar microwave scattering artifact that occurs when the signal encounters

very large wet hail. Significant power is forward-scattered such that it illuminates the ground beneath the scattering volume. Backscattered power from the ground returns to the hydrometeor region, scattering back to the radar along the same radial as the original transmission. The result, called a "flare," or TBSS, is oriented along radar radials beyond the highly reflecting storm core, and is characterized by generally weak reflectivities (normally <20 dBZ). When visible downrange of the core and depending on display thresholds, it is normally less than ~15 km in length.

Doppler velocity associated with the signature result from a complex spectrum composed of both radial and vertical motions. Only at the first TBSS radar gate are radial velocities significantly meaningful, but even these are not typically operationally useful. Under certain circumstances, accurate vertical motion estimates of the reflecting hydrometeors can be obtained. However, owing to the fact that many downrange gates are characterized by broad noiselike spectra, most mean velocities are near zero or slightly negative due to hail fall velocities. Unfortunately when these signatures occur internally to the storm, mesocyclone or other affected signatures may be partially obscured or distorted owing to TBSS velocity and width contributions.

Use of this signature with the WSR-88D has been emphasized here because of its 10-cm wavelength. Since the signature is created by hydrometeors in the Mie scattering range, a definite wavelength dependence is noted. For this reason and observations that even large raindrops can induce three-body scattering with C-band radar (5-cm wavelength), the operational conclusions presented here are confined to S-band radars and the WSR-88D in particular.

But, most importantly, WSR-88D detection and display of this signature can be used operationally. The TBSS identification during the scanning of an intense convective storm is a sufficient but not necessary condition for large hail identification. It can be and should be safely concluded that within the reflectivity core, which has induced three-body scattering, there exists the presence of large and damaging hail. When first detected within midstorm levels in an echo overhang and/or above or surrounding a BWER, rapid, wet growth of already large hail is under way within an updraft. When an echo core is in the precipitation cascade region, the responsible hail is probably descending toward the surface on the fringe of the updraft or within downdraft. Any aircraft encounter with such a reflectivity core, either during hail growth or descent, would almost certainly be fatal in this author's opinion.

For the public warning function, the forecaster should anticipate hail equal to or greater than 2.5 cm in diameter will reach the surface within the next 10–30 min. Additionally, because most of these TBSS-accompanied storms have been found to often produce very damaging surface winds, resulting warnings should contain mention of both these threats. When the TBSS signature

resembles those illustrated in the Cashion storm and the additional examples illustrated in Figs. 5 and 6, particularly damaging conditions should be emphasized in the resulting warning.

Further research is required to refine the proposed operational applications. It is also suggested that a computer algorithm be designed and tested for automated recognition of this radar artifact.

REFERENCES

Atlas, D., and F. H. Ludlam, 1961: Multi-wavelength radar reflectivity of hailstorms. *Quart. J. Roy. Meteor. Soc.,* **87,** 523–534.

Browning, K. A., 1964: Airflow and precipitation trajectories within severe local storms which travel to the right of the winds. *J. Atmos. Sci.,* **21,** 634–639.

——, 1977: The structure and mechanisms of hailstorms. *Hail: A Review of Hail Science and Hail Suppression, Meteor. Monogr.,* No. 38, Amer. Meteor. Soc., 1–43.

——, J. Hallett, T. W. Harrold, and D. Johnson, 1968: The collection and analysis of freshly fallen hailstones. *J. Appl. Meteor.,* **7,** 603–612.

Burgess, D. W., and L. R. Lemon, 1991: Characteristics of mesocyclones detected during a NEXRAD test. Preprints, *25th Int. Conf. on Radar Meteor.,* Paris, France, Amer. Meteor. Soc., 39–42.

——, and ——, 1993: Tornado and mesocyclone development in a low shear environment: The Cashion, Oklahoma storm of June 18, 1992. Preprints, *17th Conf. on Severe Local Storms,* St. Louis, MO, Amer. Meteor. Soc., 153–157.

Crum, T. D., and R. L. Alberty, 1993: Recording, archiving, and using WSR-88D data. *Bull. Amer. Meteor. Soc.,* **74,** 645–653.

Davies-Jones, R. P., D. W. Burgess, and M. P. Foster, 1990: Test of helicity as a tornado forecast parameter. Preprints, *16th Conf. on Severe Local Storms,* Kananaskis Park, AB, Canada, Amer. Meteor. Soc., 588–592.

English, M., 1973: Alberta hailstorms. Part II: Growth of large hail in the storm. *Alberta Hailstorms, Meteor. Monogr.,* No. 36, Amer. Meteor. Soc., 37–98.

Eyerman-Torgerson, K., and R. A. Brown, 1995: The hail spike signature in the Carson, ND hailstorm of 11–12 July 1989. Preprints, *27th Conf. on Radar Meteorology,* Vail, CO, Amer. Meteor. Soc., 80–82.

Hjelmfelt, M. R., R. D. Roberts, and H. D. Orville, 1986: Observational and numerical study of a microburst line-producing storm. Preprints, *Joint Sessions 23d Conf. on Radar Meteorology and Conf. on Cloud Physics,* Snowmass, CO, Amer. Meteor. Soc., J77–J80.

Lemon, L. R., 1978: On the use of storm structure for hail identification. Preprints, *18th Conf. on Radar Meteorology,* Atlanta, GA, Amer. Meteor. Soc., 203–206.

——, 1994: Recognition of the "three-body scatter spike" as a large

hail signature. Postprints, *The First WSR-88D Users Conf.,* Norman, OK, WSR-88D Operational Support Facility, 373–388.

——, and C. A. Doswell III, 1979: Severe thunderstorm evolution and mesocyclone structure as related to tornadogenesis. *Mon. Wea. Rev.,* **107,** 1184–1197.

——, and D. W. Burgess, 1993: Supercell associated deep convergence zone revealed by a WSR-88D. Preprints, *26th Int. Conf. on Radar Meteorology,* Norman, OK, Amer. Meteor. Soc., 206–208.

——, and S. Parker, 1996: The Lahoma storm deep convergence zone: Its characteristics and role in storm dynamics and severity. Preprints, *18th Conf. on Severe Storms,* San Francisco, CA, Amer. Meteor. Soc., 70–74.

NOAA, 1991: Doppler radar meteorological observations. Part A, System concepts, responsibilities, and procedures. Federal Meteorological Handbook 11, FCM-H11CA-1991, Office of the Federal Coordinator for Meteorological Services and Supporting Research, Washington, DC, 58 pp.

Ohno, H., O. Suzuki, H. Nirasawa, M. Yoshizaki, N. Hasegawa, Y.

Tanaka, Y. Muramatsu, and Y. Ogura, 1994: Okayama downbursts on 27 June 1991: Downburst identifications and environmental conditions. *J. Meteor. Soc. Japan,* **72,** 197–222.

Srivastava, R. C., 1987: A model of intense downdraft driven by the melting and evaporation of precipitation. *J. Atmos. Sci.,* **44,** 1752–1773.

Summers, P. W., 1968: Soft hail in Alberta hailstorms. *Proc. Int. Conf. on Cloud Physics,* Toronto, ON, Canada, Amer. Meteor. Soc., 455–459.

Wakimoto, R. M., and V. N. Bringi, 1988: Dual polarization observations of microburst association with intense convection: The 20 July storm during the MIST Project. *Mon. Wea. Rev.,* **116,** 1521–1539.

Wilson, J. W., and D. Reum, 1986: ''The hail spike'': Reflectivity and velocity signature. Preprints, *23d Conf. on Radar Meteorology,* Snowmass, CO, Amer. Meteor. Soc., 62–65.

——, and ——, 1988: The flare echo: Reflectivity and velocity signature. *J. Atmos. Oceanic Technol.,* **5,** 197–205.

Zrnić, D. S., 1987: Three-body scattering produces precipitation signature of special diagnostic value. *Radio Sci.,* **22,** 76–86.